Pergamon

PII: S1359-6454(96)00369-2

Acta mater. Vol. 45, No. 6, pp. 2235–2245, 1997

Published by Elsevier Science Ltd

1359-6454/97 $17.00 + 0.00

CRACK NUCLEATION ON AN ELASTIC POLYCRYSTAL SURFACE IN A CORROSIVE ENVIRONMENT: LOW DIMENSIONAL DYNAMICAL MODELS

Z. SUO and H. YU

Mechanical and Environmental Engineering Department, Materials Department, University of California, Santa Barbara, CA 93106, U.S.A.

(Received 25 July 1996; accepted 8 October 1996)

Abstract—This paper analyses a process of crack nucleation on the surface of a ceramic subject to a stress parallel to the surface, in an environment where the ceramic evaporates slowly and deforms elastically. We formulate dynamical models of one or two degrees of freedom by combining an existing elasticity solution and a variational approach. Both grain boundary tension and elastic stress concentration cause the surface to groove along its intersections with the grain boundaries. Two behaviors are identified. If the applied stress is small, the grooves approach an invariant shape, and the ceramic erodes by gross mass loss. If the applied stress is large, the grooves sharpen into crack fronts, and the ceramic breaks by decohesion. The models relate crack nucleation threshold and time to the applied stress, surface and grain boundary tensions, chemical free energy, grain size, and kinetic parameters. Surface self-diffusion is also included in the analysis. © *1997 Acta Metallurgica Inc.*

1. INTRODUCTION

When a large enough tensile stress is applied for some time, a ceramic creeps and grows cavities at high temperatures, and breaks by slow decohesion at low temperatures. We suggest that another behavior is possible in a range of intermediate temperatures, high enough to allow mass transport on the external surface, but low enough to suppress rate processes in grains and on grain boundaries. Evaporation is one process that may operate in this intermediate temperature range. For example, solid oxides may decompose into gaseous suboxides at low oxygen partial pressure, or in the presence of hydrogen. Such reactions and other solid–gas reactions have been observed in sintering [1].

Figure 1 illustrates the geometry to be analysed. A polycrystal, with a periodic array of grains on an external surface, is in contact with a vapor, and subject to a stress parallel to the surface. The solid is two dimensional, semi-infinite, and elastic. At any time, the temperature is uniform throughout, the partial pressure of every molecular species is uniform in the vapor, and a static elastic field prevails in the solid. The solid and the vapor, however, are not in chemical equilibrium with each other, and the solid evaporates to the vapor. It is well known that grain boundary tension causes mass to evaporate preferentially along the intersections between the external surface and the grain boundaries, leaving grooves on the surface. This paper analyses the additional effects of the applied stress. The elastic energy density is nonuniform on the surface, concentrating at the groove roots. Two behaviors are expected. If the applied stress is small, the grooves approach an invariant shape, and the ceramic erodes by gross mass loss. If the applied stress is large, the grooves sharpen into crack fronts, and the ceramic breaks by decohesion. Although several related phenomena have been discussed in the literature (see below), we are unaware of models or experiments that elucidate this crack nucleation process on the polycrystal surface. Many ceramic components are used at such intermediate temperatures and corrosive environments, and the phenomenon may limit their lifetimes.

Hillig and Charles [2] reviewed early studies on the relationship between dissolution and strength, mainly for glasses. They assumed in their model that notch-like flaws exist on the glass surface. If the rate of dissolution is uniform on the surface, the flaw tip will blunt. The strengthening of glass by etching in hydrofluoric acid can be explained in this way. However, if a stress is applied and the dissolution rate is stress enhanced, the flaw tip may sharpen. The process can lead to static fatigue of glass. Later work showed that stress-assisted mass transport can destabilize an external surface [3] and an internal pore [4], changing the surface shape to nucleate crack fronts [5–7]. Similar stress-assisted morphological instabilities in epitaxial films and composites have been reviewed elsewhere [8, 9].

Of particular importance to this paper is the work of Chiu and Gao [5]. They approximated a wavy single crystal surface by a cycloid, and solved the exact elastic field in the crystal. As the amplitude-to-wavelength ratio varies, the cycloid varies from a

straight line to a wavy curve with crack-like troughs. These authors used the family of cycloids to study the energetics of an evolving surface, and aspects of kinetics assuming surface diffusion.

Elasticity field in a body of an arbitrary shape is difficult to determine accurately. Consequently, analytic elasticity solutions for idealized geometries (e.g. slits, ellipses, and cycloids) are valuable, as they approximate more complex geometries and allow phenomena to be understood in simple terms. In previous papers [10, 11], we have developed an approach to constructing dynamical systems on the basis of any geometric model. This paper approximates an evolving polycrystal surface by cycloids, and formulates dynamical systems of one and two degrees of freedom. Self-diffusion and reaction on the polycrystal surface are considered separately as the mass transport processes.

Two points need to be clarified before we proceed with the formulation. First, grain arrays similar to Fig. 1 were analysed recently under the assumption that mass diffuses on the grain boundaries, as well as on the external surface [12, 13]. In those analyses, the grains were taken to be rigid, and the applied stress does work to moving grains relative to one another, accommodating mass inserted into or removed from the grain boundaries. Because mass diffuses on the grain boundaries, the stress distribution along the grain boundary differs greatly from that of an elastic stress concentrator. Although surface diffusion usually operates at similar temperatures to grain boundary diffusion, in this paper we include the model with surface diffusion but no grain boundary diffusion. The model is used for comparison with existing ones for single crystals, and to make several conceptual points. It may also be a useful limiting case when the surface diffusivity is much greater than the grain boundary diffusivity.

Second, if the proposed failure process happens, a ceramic component under a stress exceeding the threshold would spend its lifetime mainly in two stages [7]. In stage I, the grooves change shape to nucleate crack fronts. In stage II, the cracks extend by slow decohesion to attain the critical size for fast fracture. Different kinetic processes may limit the rates in the two stages, and one stage may take a much longer time than the other. In this connection, micrographs could be deceptive. For a crack front to nucleate, the overall surface shape changes a little and may be difficult to see, as compared to a possibly large surface area created by slow decohesion. However, the time for crack nucleation need not be shorter than the time for crack extension. Such a time of little overall geometric change (stage I) may well identify with the incubation time in an experimental observation. Mass transport and slow decohesion have different temperature dependencies. Also, shape change is driven by the variation in the elastic energy, which operates under both tensile and compressive stress, but decohesion requires tensile stress. These differences can help to distinguish the two processes experimentally.

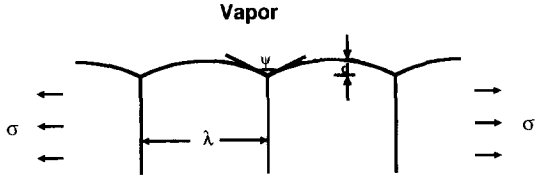

Fig. 1. Semi-infinite elastic polycrystal, in contact with a vapor, subject to a stress parallel to the surface.

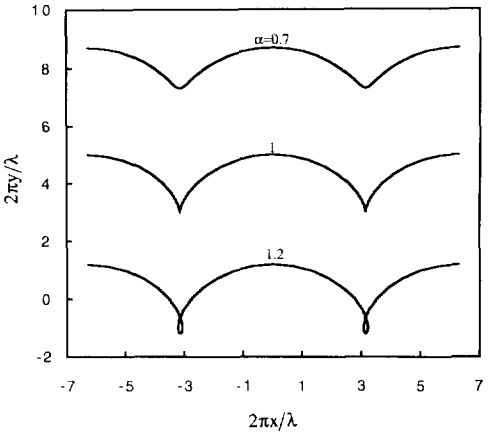

Fig. 2. Cycloids of several amplitude-to-wavelength ratios.

2. GEOMETRY AND ENERGY

Following Ref. [5], we now briefly describe the geometry of a cycloid. A cycloid is the trajectory of a point fixed on a circular disk which rolls without slipping on a horizontal surface. The disk radius, R, is used to normalize other lengths. Denote the distance between the fixed point and the disk center by αR. The x-axis is parallel to the horizontal surface, and the y-axis vertical; the disk center lies at a distance βR above the x-axis. For a fixed set (R, α, β), as the disk rolls by an angle θ, the point fixed on the disk moves to a position of coordinates

$$x = (\theta + \alpha \sin\theta)R, \quad y = (\beta + \alpha \cos\theta)R. \quad (1)$$

These equations describe the cycloid, with θ as the variable parameter. Figure 2 shows several cycloids. The height of the disk center is arbitrarily placed. When the fixed point lies at the disk center, the cycloid degenerates to a straight line. When the fixed point lies inside the disk but off center, $0 < \alpha < 1$, the cycloid is a smooth wavy curve of wavelength $\lambda = 2\pi R$, and crest-to-trough amplitude $2\alpha R$. When the fixed point lies on the perimeter of the disk, $\alpha = 1$, the cycloid has crack-like troughs, with parallel tangents approaching from two sides of each trough. When the fixed point lies outside the disk, $\alpha > 1$, the cycloids have loops. Additional geometric relationships are collected in the Appendix.

Approximate the cross-section of an evolving polycrystal surface by a family of cycloids in the range $0 \leqslant \alpha \leqslant 1$. Identify the wavelength $\lambda = 2\pi R$ with the grain size, and the amplitude $2\alpha R$ with the groove depth. The grain boundaries are at $\theta = \pm\pi, \pm 3\pi, \ldots$. Take a polycrystal with a flat surface ($\alpha = \beta = 0$) as the reference energy state. Given below are the excess energies per grain per unit thickness.

The surface tension γ_S and the grain boundary tension γ_B are taken to be isotropic. The surface energy per unit thickness equals γ_S times the curve length. The length per period of a cycloid is computed by integrating equation (A3). Consequently, the excess energy per grain surface is

$$U_S = \gamma_S R\left[\int_0^{2\pi} (1 + 2\alpha\cos\theta + \alpha^2)^{1/2}\,d\theta - 2\pi\right]. \quad (2)$$

The vertical coordinate of the groove root is $y_{\theta=\pi} = R(\beta - \alpha)$. Thus, the excess energy per grain boundary is

$$U_B = \gamma_B R(\beta - \alpha). \quad (3)$$

The free energy increase per unit volume of solid condensed from the vapor on a flat, stress-free solid surface, g, can be calculated from the reference chemical potentials of the solid and the gases, and the partial pressures of the gases. The solid is assumed to be immersed in such a large amount of the gases that the chemical potentials of the gases change negligibly during the reaction. Thus, g is constant in this model. The excess chemical energy is g times the area under the cycloid:

$$U_C = \pi g R^2(2\beta + \alpha^2). \quad (4)$$

We have used equation (A4) for the area under each period of the cycloid.

Now consider the elastic energy difference between the body with a flat surface and the body with a grooved surface, each subject to a horizontal stress. The displacement at the loading point is held constant, so that the loading device does no work to the ceramic as the surface evolves. Assume that mass attaches to the solid surface coherently without creating dislocations or other stress-relieving defects. The elastic energy increases when mass is added onto the traction-free surface, and decreases when the grooves deepen. The exact elastic field in a half plane bounded by a cycloid is available [5]. The excess elastic energy per grain under the plane stress condition is

$$U_E = \frac{\pi R^2\sigma^2}{2E}(2\beta - \alpha^2). \quad (5)$$

Under the plane strain conditions, replace E by $E/(1-\nu^2)$, where E is Young's modulus, and ν Poisson's ratio.

The total excess energy per unit thickness per grain is

$$G = U_S + U_B + U_C + U_E. \quad (6)$$

Three dimensionless groups measure the significance of the grain boundary tension, the chemical free energy, and the elastic energy relative to the surface tension:

$$\Gamma = \frac{\gamma_B}{\gamma_S}, \quad \chi = \frac{g\lambda}{\gamma_S}, \quad \Lambda = \frac{\sigma^2\lambda}{E\gamma_S}. \quad (7)$$

Because the last two groups involve ratios of energy per volume to energy per area, the grain size λ enters both.

The dimensionless groups are independent of the cycloid model, and are inherent to the phenomenon. Their qualitative significance is readily understood. Imagine a three dimensional space formed by using the values of Γ, χ, and Λ as the coordinates. When $\Gamma > 2$, the free energy reduces as two free surfaces replace one grain boundary, so that a triple junction loses local equilibrium and atomic bonds break spontaneously along the grain boundary under no applied stress. Our model will be restricted in the region $0 \leqslant \Gamma \leqslant 2$. The normalized chemical free energy, χ, may take any value. When $\chi > 0$, a solid with a flat, stress-free surface has a higher free energy than the vapor, and the solid evaporates. When $\chi < 0$, a solid with a flat, stress-free surface has a lower free energy than the vapor, and the solid condenses. A solid surface, if curved or under stress, evaporates or condenses even when $\chi = 0$, depending on the total free energy G. The normalized load can take any value $\Lambda \geqslant 0$, and tends to destabilize grooves. A surface divides the parameter space (Γ, χ, Λ) into two regions. A polycrystal subject to a condition in one region will groove into an invariant shape; in another region, into crack fronts. This dividing surface is the threshold for crack nucleation, to be deduced from our models.

3. SURFACE DIFFUSION

This section assumes that atoms only diffuse on the surface. Because no mass exchanges between the solid and the vapor, U_C does not enter this process. The solid conserves mass, so that $\beta = -\alpha^2/2$ according to equation (A4). The dynamical system has only one degree of freedom; we use the dimensionless groove depth, α, as the generalized displacement.

3.1. *Energetics*

When the solid conserves mass, the total excess energy becomes

$$\frac{G}{\lambda\gamma_S} = \frac{1}{2\pi}\int_0^{2\pi} (1 + 2\alpha\cos\theta + \alpha^2)^{1/2}\,d\theta - 1 - \frac{\Gamma}{2\pi}\left(\frac{\alpha^2}{2} + \alpha\right) - \frac{\Lambda\alpha^2}{4\pi}. \quad (8)$$

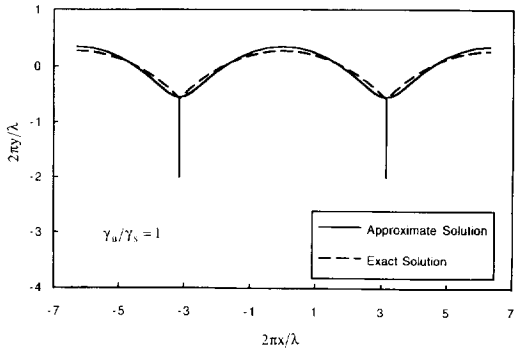

Fig. 3. Comparison of the exact and approximate equilibrium groove shapes. No stress is applied.

This gives the free energy as a function of the generalized displacement, $G(\alpha)$.

First examine the familiar situation where no stress is applied, $\Lambda = 0$. Under the action of surface and grain boundary tensions, the grooves approach an equilibrium shape, the exact solution of which is well known: each grain surface is a circular arc of radius λ/Γ; the two grain surfaces meet at a triple junction by a dihedral angle Ψ, determined by $\cos(\Psi/2) = \Gamma/2$; within the cycloid model, the approximate equilibrium shape is determined by minimizing the energy function $G(\alpha)$. Figure 3 compares the exact and the approximate equilibrium shapes for $\Gamma = 1$. The overall shapes agree well, and better agreement is found for smaller values of Γ. Figure 4 compares the depths of the exact and the approximate equilibrium grooves. They agree well except for very large grain boundary tensions. These comparisons give some confidence in approximating polycrystal surfaces by cycloids.

Certain local details are inadequately represented by a cycloid. In particular, the exact solution has the dihedral angle $\Psi = 120$ at $\Gamma = 1$ as dictated by local equilibrium, but the approximate solution is flat at the groove root as dictated by a cycloid of $\alpha < 1$. Local discrepancies like this is often encountered

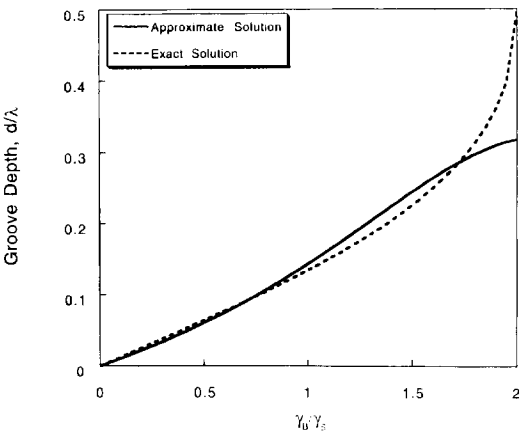

Fig. 4. Comparison of exact and approximate equilibrium groove depths as a function of Γ. No stress is applied.

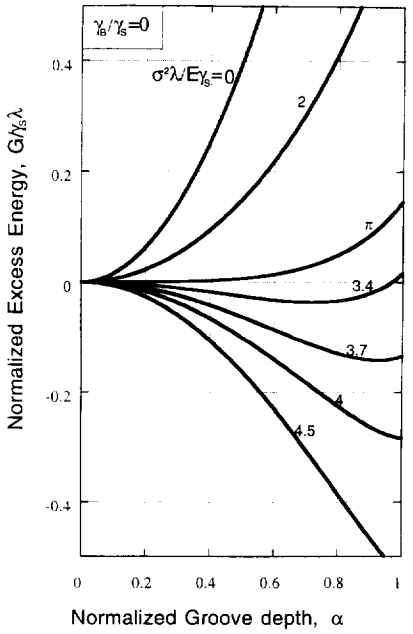

Fig. 5. Free energy as a function of generalized displacement ($\Gamma = 0$). The solid conserves mass.

when approximating a system of many degrees of freedom by a model of a few degrees of freedom, and should not cause excessive concerns if one only looks for global behaviors of the system.

We next examine the effect of stress. When the grain boundary tension is negligibly small compared to the surface tension, $\Gamma \to 0$, our results reproduce those in Ref. [5] for a single crystal surface. Figure 5 plots $G(\alpha)$ at $\Gamma = 0$ and several levels of Λ. For a small applied stress ($0 \leqslant \Lambda < \pi$), the energy increases with the groove depth, and the flat surface ($\alpha = 0$) is a stable equilibrium state. For an intermediate applied stress ($\pi < \Lambda < 4$), the energy first decreases, reaches a minimum, and then increases as the groove deepens, so that the flat surface is an unstable equilibrium state and the surface can form a stable equilibrium groove. For a large applied stress ($\Lambda > 4$), the energy decreases in the entire range of groove depth, so that the flat surface is an unstable equilibrium state and a crack front will nucleate.

Figure 6 plots the function $G(\alpha)$ at $\Gamma = 0.5$ and several levels of Λ. As expected, the flat surface is not in equilibrium even under no applied stress. For a small applied stress ($0 \leqslant \Lambda < 3$), the energy minimizes at a certain value of $\alpha < 1$, so that a groove approaches an equilibrium state. For a large applied stress, $\Lambda > 3$, the energy decreases in the entire range of groove depth, and a crack front nucleates.

We calculate the equilibrium groove depth by minimizing the energy function $G(\alpha)$ in $0 \leqslant \alpha \leqslant 1$. Figure 7 gives the equilibrium load–displacement diagram. Each curve represents, for a given value of Γ, the equilibrium groove depth, α, as a function of the load level, Λ. All curves end when the crack nucleates, $\alpha = 1$. The case $\Gamma = 0$ shows a supercritical

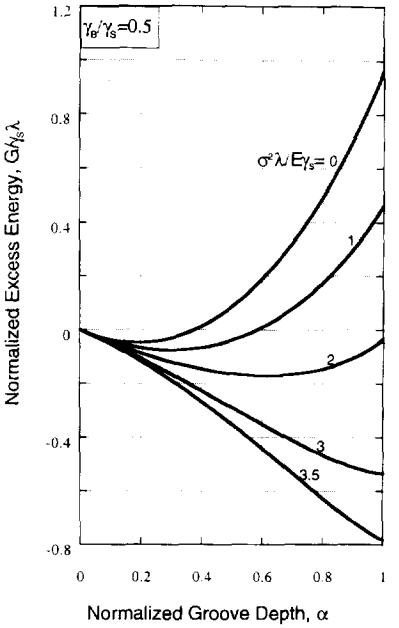

Fig. 6. Free energy as a function of generalized displacement ($\Gamma = 0.5$). The solid conserves mass.

pitchfork bifurcation at $\Lambda = \pi$: the flat surface is in a stable equilibrium state when $\Lambda < \pi$, and in an unstable equilibrium state when $\Lambda > \pi$; a sequence of stable equilibrium grooves exist when $\pi < \Lambda < 4$. The bifurcation point $\Lambda = \pi$ can be obtained by linear stability analysis [3, 14]. When $\Gamma > 0$, the grain boundary tension causes the surface to groove even when no stress is applied ($\Lambda = 0$). For a fixed value of Γ, the equilibrium groove depth increases as the load Λ increases.

All equilibrium load–displacement curves in Fig. 7 increase up to crack nucleation, $\alpha = 1$. For a given value of Γ, cracks will not nucleate if the applied load Λ is below its equilibrium value at $\alpha = 1$. Consequently, this value represents the threshold for crack nucleation. At $\alpha = 1$, the equilibrium condition, $dG/d\alpha = 0$, determines the threshold load

$$(\sigma^2\lambda/E)_{th} = 2(2\gamma_S - \gamma_B). \tag{9}$$

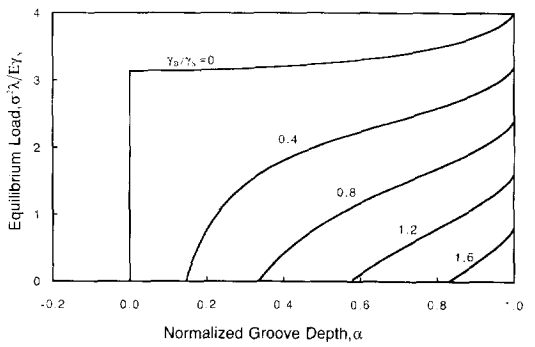

Fig. 7. Equilibrium load–displacement curves at several values of Γ. The solid conserves mass.

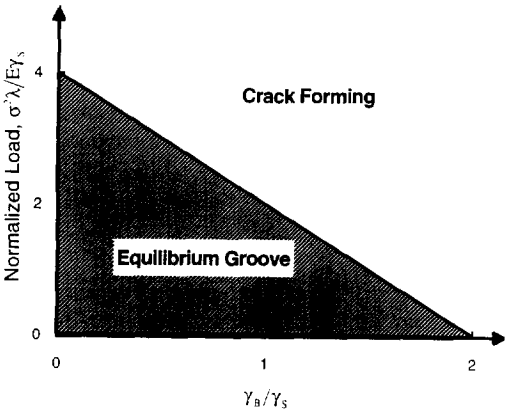

Fig. 8. Parameter plane (Γ, Λ) divided into two regions by a line (the threshold). Under a condition below the threshold, a polycrystal surface approaches at an equilibrium shape; above, the surface nucleates cracks. The solid conserves mass.

This corresponds to a straight line that divides the parameter plane (Γ, Λ) into two regions (Fig. 8). Under a condition below the line, a polycrystal surface approaches equilibrium grooves; above it, the surface nucleates cracks. The two limiting points on the dividing line are known previously. At $\Gamma = 2$, the triple junction loses local equilibrium under no applied stress. At $\Gamma = 0$, the grain boundary tension is negligible compared to the surface tension, so that the polycrystal surface is similar to a single crystal surface, which grooves into cracks if $\Lambda = 4$, as predicted in Ref. [5]. Except for the point ($\Gamma = 2$, $\Lambda = 0$), the dividing line is a consequence of the cycloid geometry, and one should not attach any significance to the exact form of the line (e.g. its being a straight line, or $\Lambda = 4$ at $\Gamma = 0$). We believe, however, that this line is close to the exact solution, because the exact subcritical groove shapes are expected to be well approximated by the cycloids.

Everything else being fixed, the threshold stress decreases as the grain size increases according to $\sigma_{th} \propto \lambda^{-1/2}$. The conclusion is reasonable for a polycrystal where grain boundary grooves are the dominant surface imperfections. Obviously the rule has to break down when grain size is very small, and other imperfections become relatively large. As is evident in Fig. 6, for a given subcritical value of Λ, the grain size scales the depth of the free energy well, which determines the ability of the well to trap the polycrystal surface. When the grain size is too small, the energy well may be removed by the presence of other larger imperfections. In this case, the small grain size no longer gives rise to a large threshold stress, and cracks can nucleate from the larger imperfections. Models of more degrees of freedom are needed to study this effect.

3.2. *Dynamics*

We now formulate a dynamical model using a variational approach. Imagine that the surface

changes shape slightly as a small amount of mass relocates along the surface. Let δI be the small mass displacement (i.e. the number of atoms crossing per unit length on the surface). An element of the grain surface ds moves in the direction normal to the element by a small distance δr_n. Mass conservation requires that

$$\delta r_n + \Omega\, \partial(\delta I)/\partial s = 0 \tag{10}$$

where Ω is the volume per atom. The small mass displacement and the surface movement required by mass conservation describe a virtual change in the system state, a change that need not obey any kinetic law. Associated with the virtual change, the free energy varies by δG.

For any virtual state change, the actual atomic flux J (i.e. the number of atoms per unit time crossing per length on the surface) satisfies the weak statement [e.g. 10, 15]

$$\int \frac{J\delta I}{M}\, ds = -\delta G. \tag{11}$$

The integral extends over one grain surface. The atomic mobility on the surface, M, obeys the Einstein relation,

$$M = \frac{D_s \delta_s}{\Omega k T} \tag{12}$$

where D_s is the surface self-diffusivity, δ_s the thickness of atomic layers participating in surface diffusion, k the Boltzmann constant, and T the absolute temperature. The diffusivity varies with the temperature according to the Arrhenius law $D_s = D_{s0}\exp(-q/kT)$, where q is the activation energy.

We next apply the weak statement to the cycloid model. The dimensionless groove depth α is the generalized displacement of the dynamical system, its time rate $\dot{\alpha}$ is the generalized velocity, and its variation $\delta\alpha$ describes the virtual change of the system state. To conserve solid mass, $\delta\beta = -\alpha\delta\alpha$. The free energy varies by $\delta G = -f\delta\alpha$. The generalized force f is calculated by taking the derivative of G in equation (8), namely

$$\frac{f}{R\gamma_s} = -\int_0^{2\pi} \frac{(\alpha + \cos\theta)\, d\theta}{(1 + 2\alpha\cos\theta + \alpha^2)^{1/2}} + \Gamma(1 + \alpha) + \Lambda\alpha. \tag{13}$$

Using the expression for δr_n in equation (A8), and integrating equation (10), we obtain

$$\delta I = \left[-\frac{R^2}{\Omega}(1 - \alpha^2)\sin\theta\right]\delta\alpha. \tag{14}$$

We have used the symmetry condition $\delta I = 0$ at $\theta = 0$. Mass conservation requires that the flux J and the normal velocity of the surface, v_n, obey a relation similar to equation (10). Consequently, J relates to the generalized velocity in the same way as equation (14), namely,

$$J = \left[-\frac{R^2}{\Omega}(1 - \alpha^2)\sin\theta\right]\dot{\alpha}. \tag{15}$$

Inserting the above into the weak statement (11), we obtain

$$H\dot{\alpha} = f. \tag{16}$$

The generalized viscosity is given by

$$H = \frac{R^5(1 - \alpha^2)^2}{M\Omega^2}\int_0^{2\pi} \sin^2\theta(1 + 2\alpha\cos\theta + \alpha^2)^{1/2}\, d\theta. \tag{17}$$

Since both H and f depend on α, equation (16) is a nonlinear ordinary differential equation, which we integrate numerically.

Figure 9 plots the groove depth as a function of time for $\Gamma = 0.5$ and several levels of Λ. (When $\Gamma = 0.5$, the threshold load is $\Lambda_{th} = 3$.) In the calculation, we have assumed that initially the surface is flat. The surface approaches an equilibrium state under a subcritical condition, but nucleates crack fronts under a supercritical condition. As a supercritical groove sharpens, its velocity diverges. Once the crack front forms, its velocity is no longer limited by self-diffusion; other processes must be invoked to limit its velocity, such as stress wave propagation, or impurity transport needed to lower the surface tension of the freshly created surfaces. Decohesion after crack nucleation is not studied in this paper.

For a polycrystal subject to a condition above the threshold in the parameter plane (Γ, Λ), an initially flat polycrystal surface takes a finite amount of time, t_N, to nucleate cracks. A dimensional analysis shows that

$$t_N = \frac{\lambda^4}{(2\pi)^4 M\Omega^2\gamma_s}\tau(\Gamma, \Lambda) \tag{18}$$

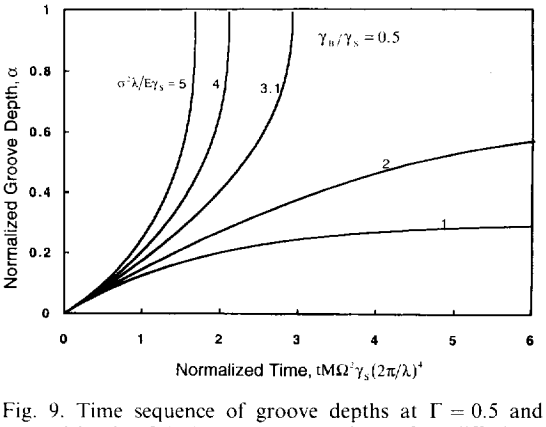

Fig. 9. Time sequence of groove depths at $\Gamma = 0.5$ and several levels of Λ. Mass transports by surface diffusion.

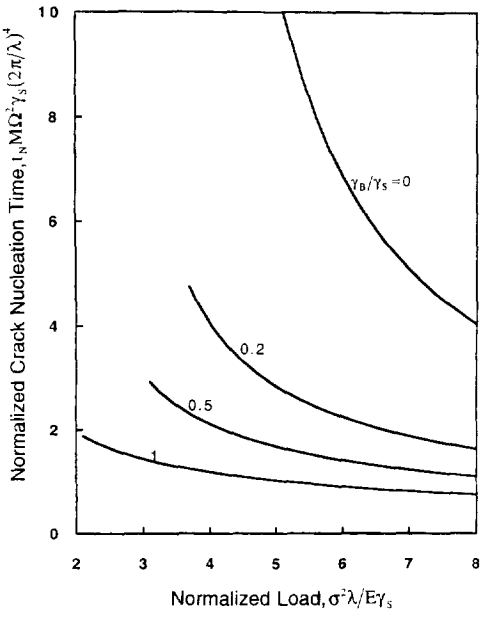

Fig. 10. Time needed for an initially flat polycrystal surface to nucleate crack fronts by surface diffusion, subject to conditions above the threshold on (Γ, Λ) plane.

where $\tau(\Gamma, \Lambda)$ is a dimensionless function, decreasing as Γ or Λ increases. The list of independent variables should also include those describing the initial surface geometry; special cases are considered below. This functional form is independent of the cycloid model, and is inherent to the phenomenon. The crack nucleation time depends on the temperature through the mobility. Figure 10 plots the nucleation time computed from the model. For $\Gamma = 0$, the flat surface is an unstable equilibrium state, and the calculation was initiated with a slightly undulating surface, $\alpha = 10^{-3}$. For $\Gamma > 0$, the flat surface is in a nonequilibrium state, and the calculation was initiated at $\alpha = 0$. The normalization for time in Fig. 10 is consistent with equation (18), which readily compares crack nucleation times for polycrystals of a fixed grain size under different stress levels. The effect of grain boundary tension is also evident in Fig. 10.

The trends of the curves in Figs 9 and 10 are as expected. However, we do not believe that the cycloid model adequately predicts the crack size and the nucleation time under conditions much above the threshold. Under such a condition, the groove roots should localize within a length much smaller than the grain size, leading to a shorter crack size and a shorter nucleation time than predicted by the cycloid model. In a separate paper, we shall use models of many degrees of freedom to compute the crack nucleation time.

4. EVAPORATION–CONDENSATION

At least two degrees of freedom are needed to describe an evolving surface under evaporation–condensation: one for overall mass loss or gain, and the other for the shape change. The parameters, β and α, serve these two purposes, respectively. When no stress is applied, the surface approaches an invariant shape, moving steadily, as the solid evaporates or condenses under the action of the surface tension, the grain boundary tension, and the chemical free energy. When a small stress is applied to the solid, the surface approaches a different steady shape. When a large stress is applied, the surface can never reach steady shape, but nucleates crack fronts. In all cases, except for the special situation where evaporation just balances condensation, the system never reaches equilibrium. In such a problem, free energy alone does not determine the stability of the steady state. Within the cycloid model, the free energy is a function of two generalized displacements, $G(\alpha, \beta)$. In what follows we formulate a dynamical system of two degrees of freedom.

The process of evaporation involves several steps. Reactant molecules diffuse in the vapor to the solid, react with the solid at appropriate surface sites, and product molecules diffuse in the vapor away from the solid. The detailed kinematic process is uncritical to us in this work. In the following calculation, we assume that the surface reaction step limits the rate of evaporation.

Imagine that an element of the grain surface ds moves by a small amount δr_n in the direction normal to the surface element as a small amount of mass is added to or removed from the solid. The free energy, G, now includes all four terms in equation (6). For any virtual motion, the actual normal velocity of the surface, v_n, satisfies the weak statement [e.g. 11, 15]

$$\int \frac{v_n \delta r_n}{m} \, ds = -\delta G \tag{19}$$

where m is the specific evaporation–condensation rate (i.e. the velocity of the solid surface driven at unit free energy reduction per unit solid volume of evaporation or condensation). In this paper we assume that m is independent of stress, and is constant in the model. The integral extends over one grain surface.

Describe the small change in the surface by $\delta\alpha$ and $\delta\beta$. The free energy function $G(\alpha, \beta)$ varies by

$$\delta G = -f_\alpha \delta\alpha - f_\beta \delta\beta. \tag{20}$$

The generalized forces, $f_\alpha = -\partial G/\partial\alpha$ and $f_\beta = -\partial G/\partial\beta$, are given by

$$\frac{f_\alpha}{\gamma_S R} = -\int_0^{2\pi} \frac{(\alpha + \cos\theta)\, d\theta}{(1 + 2\alpha\cos\theta + \alpha^2)^{1/2}} + \Gamma - \alpha\chi + \frac{\alpha\Lambda}{2} \tag{21a}$$

$$\frac{f_\beta}{\gamma_S R} = -\Gamma - \chi - \frac{\Lambda}{2}. \tag{21b}$$

The virtual displacement δr_n relates to $\delta\alpha$ and $\delta\beta$ as given by equation (A8). The normal surface

velocity relates to the generalized velocities in a similar way:

$$v_n = R^2(\alpha + \cos\theta)\frac{\partial\theta}{\partial s}\dot{\alpha} + R^2(1 + \alpha\cos\theta)\frac{\partial\theta}{\partial s}\dot{\beta}. \quad (22)$$

Substituting the above into the weak statement (19), and noting that $\delta\alpha$ and $\delta\beta$ vary independently, we obtain

$$\begin{bmatrix} H_{\alpha\alpha} & H_{\alpha\beta} \\ H_{\beta\alpha} & H_{\beta\beta} \end{bmatrix}\begin{bmatrix} \dot{\alpha} \\ \dot{\beta} \end{bmatrix} = \begin{bmatrix} f_\alpha \\ f_\beta \end{bmatrix} \quad (23)$$

with the generalized viscosities being

$$H_{\alpha\alpha} = \frac{R^3}{m}\int_0^{2\pi} \frac{(\alpha + \cos\theta)^2\,d\theta}{(1 + 2\alpha\cos\theta + \alpha^2)^{1/2}} \quad (24a)$$

$$H_{\alpha\beta} = H_{\beta\alpha} = \frac{R^3}{m}\int_0^{2\pi} \frac{(1 + \alpha\cos\theta)(\alpha + \cos\theta)\,d\theta}{(1 + 2\alpha\cos\theta + \alpha^2)^{1/2}} \quad (24b)$$

$$H_{\beta\beta} = \frac{R^3}{m}\int_0^{2\pi} \frac{(1 + \alpha\cos\theta)^2\,d\theta}{(1 + 2\alpha\cos\theta + \alpha^2)^{1/2}}. \quad (24c)$$

Inverting equation (23), we have

$$\dot{\alpha} = \frac{H_{\beta\beta}f_\alpha - H_{\alpha\beta}f_\beta}{H_{\alpha\alpha}H_{\beta\beta} - H_{\alpha\beta}^2}, \quad (25a)$$

$$\dot{\beta} = \frac{H_{\alpha\alpha}f_\beta - H_{\alpha\beta}f_\alpha}{H_{\alpha\alpha}H_{\beta\beta} - H_{\alpha\beta}^2}. \quad (25b)$$

This is a set of nonlinear ordinary differential equations for the two generalized displacements. Both the viscosity matrix and the force column depend on α but not on β, so that equation (25a) can be integrated independently from (25b).

A steady state is obtained when $\dot{\alpha} = 0$, which requires that

$$H_{\beta\beta}f_\alpha - H_{\alpha\beta}f_\beta = 0. \quad (26)$$

This equation determines the steady state value of the normalized groove depth, α_{ss}, for a given set (Γ, χ, Λ). The solution must be restricted in the range $0 \leqslant \alpha_{ss} \leqslant 1$. Once α_{ss} is solved, equation (25b) determines the steady state velocity of the polycrystal surface in the vertical direction.

First examine the case $\Lambda = \chi = 0$. The solid surface recedes as solid mass evaporates under the action of the grain boundary and the surface tensions. The exact solution is known for this case. In the steady state the groove depth d and the grooving velocity V are [15]

$$\frac{d}{\lambda} = \frac{\ln\left(\sin\frac{\Psi}{2}\right)}{\pi - \Psi}, \quad V = \frac{m\gamma_s}{\lambda}(\pi - \Psi). \quad (27)$$

This exact solution is compared to the approximate solution obtained from the cycloid model in Fig. 11. They agree well for a large range of Γ.

Next examine the steady state solutions when Λ and χ do not vanish. Equation (25a) can be written as

$$\dot{\alpha} = B[\Lambda - (C_1 + C_2\Gamma + C_3\chi)] \quad (28)$$

where C_1, C_2, C_3, and B only depend on α. This form of the evolution equation explicitly shows the role of Λ, Γ, and χ. Recall that Λ, if acting alone, would cause the groove to grow, so that $B > 0$. In the steady state, i.e. $\alpha = \alpha_{ss}$ and $\dot{\alpha} = 0$, the quantity in the bracket vanishes, i.e.

$$\Lambda = C_1(\alpha_{ss}) + \Gamma C_2(\alpha_{ss}) + \chi C_3(\alpha_{ss}).$$

This gives the relationship between the load (Λ) and the steady state displacement (α_{ss}). Figure 12 plots this relationship for $\Gamma = 0.5$ and several values of χ. Under a strong evaporation condition (i.e. a large positive χ), the load Λ reaches the maximum when the crack front forms ($\alpha = 1$). Under a strong condensation condition (i.e. a large negative χ), the load reaches the maximum before the crack front forms ($\alpha < 1$).

The significance of the maximum is as follows. Focus on one curve in Fig. 12, e.g. the one for $\chi = -100$. For a given load level Λ just below the maximum, two steady states exist. We now show that the steady state on the left is stable, and the one on the right is unstable. For a steady state to be stable, the derivative of the right-hand side of equation (28)

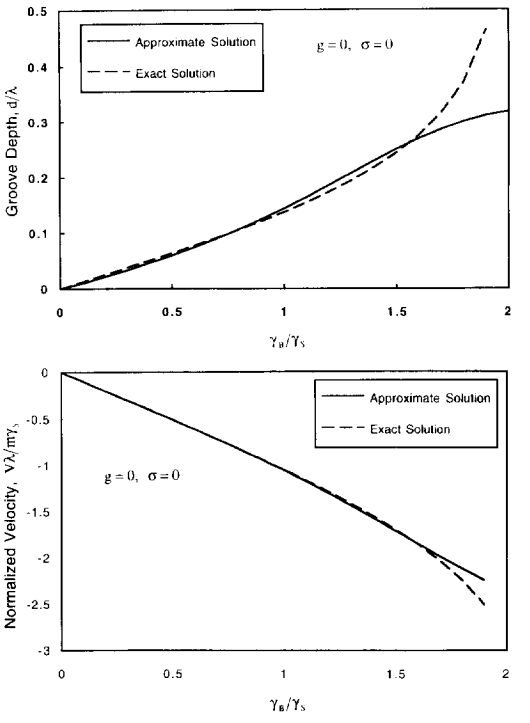

Fig. 11. Comparison between exact and approximate steady state grooves by evaporation under the condition $\chi = \Lambda = 0$. (a) Groove depth as a function of Γ. (b) Steady velocity as a function of Γ.

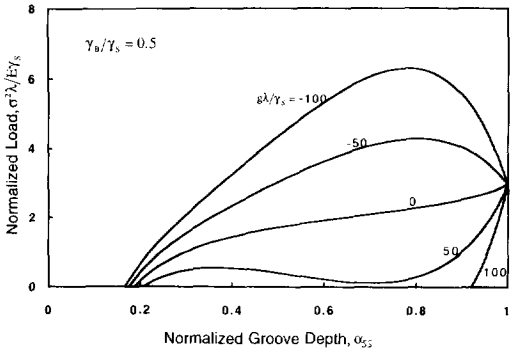

Fig. 12. Steady state load–displacement diagram.

with respective to α, taken at $\alpha = \alpha_{ss}$, must be negative:

$$\frac{dB}{d\alpha}[\Lambda - (C_1 + C_2\Gamma + C_3\chi)] - B\frac{d}{d\alpha}(C_1 + C_2\Gamma + C_3\chi) < 0.$$

When $\alpha = \alpha_{ss}$, the first bracket vanishes, and the stability condition becomes

$$\frac{d}{d\alpha}(C_1 + C_2\Gamma + C_3\chi) > 0.$$

Consequently, the steady states on the rising part of the load–displacement curve in Fig. 12 are stable, and those on the falling part are unstable.

Observe that all curves in Fig. 12 end at point ($\alpha_{ss} = 1$, $\Lambda = 3$). At this point, the polycrystal surface forms cracks. Once the cracks form, their extension does not require the solid to exchange mass with the vapor, so that the normalized chemical free energy, χ, drops out of the energetic competition. The fixed crack size, $\alpha_{ss} = 1$, however, is an artifact of the cycloid model, and would change if more degrees of freedom are allowed.

The maximum loads in Fig. 12 are the threshold for crack nucleation. Figure 13 plots the threshold as a function χ and Γ. For a fixed value of Γ, the corresponding line in Fig. 13 distinguishes two behaviors. The polycrystal surface moves by an invariant shape under a condition below the line, and nucleates cracks under a condition above the line. The threshold load, Λ_{th}, increases when the vapor condenses, and remains nearly constant when the solid evaporates.

Figure 14 plots the time sequence of the groove depths. Under a subcritical condition, an initially flat surface changes shape and simultaneously exchanges mass with the vapor, approaching a steady state with an invariant shape and a constant speed. Under a supercritical condition, the groove sharpens to a crack front, and its velocity diverges.

Under a condition above the threshold, represented by a point above the dividing surface in the (Γ, χ, Λ) surface, an initially flat polycrystal surface

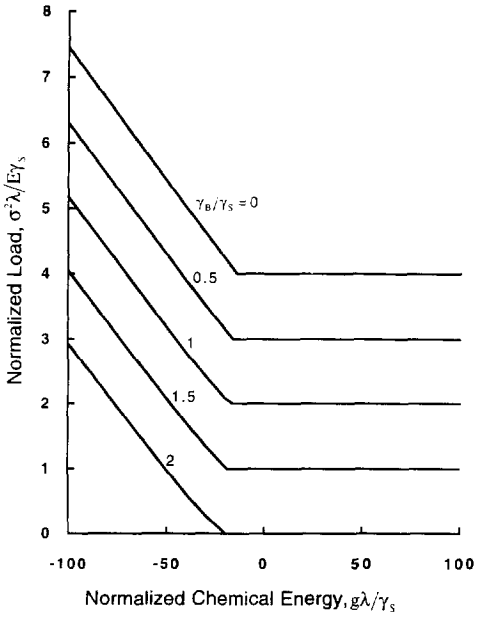

Fig. 13. Parameter (Γ, χ, Λ) space divided into two regions by a surface (the threshold). The diagram gives constant Γ lines of the dividing surface.

nucleates cracks in finite time. The nucleation time takes the form

$$t_N = \frac{\lambda^2}{(2\pi)^2 m\gamma_S}\tau(\Gamma, \chi, \Lambda) \tag{29}$$

where $\tau(\Gamma, \chi, \Lambda)$ is a dimensionless function. Again, the nucleation time depends on the initial surface geometry. Figure 15 plots the nucleation time computed from the model, assuming that the surface is initially flat.

We should make similar cautionary remarks about the model for two degrees of freedom. Subject to evaporation–condensation, a large value of $|\chi|$ alone should localize a groove root within a length scale much smaller than the grain size. This in turn should affect the numerical predictions of all quantities, including the threshold, the nucleation time, and the crack size. More degrees of freedom are necessary to describe a localized groove. A generalization of the cycloid model is under

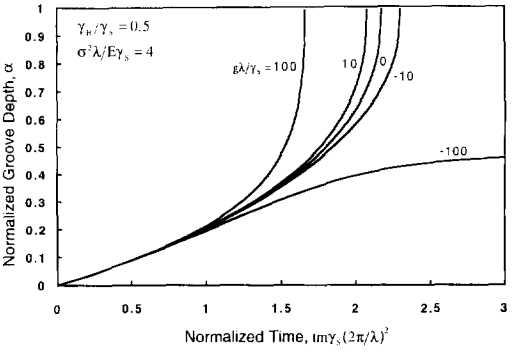

Fig. 14. Time sequences of groove depths.

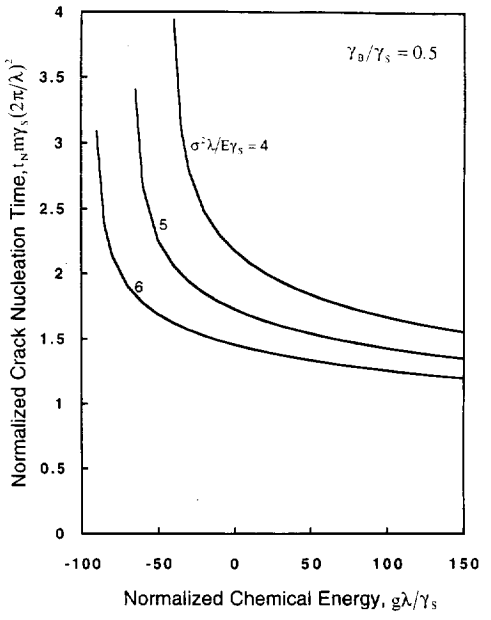

Fig. 15. Time needed for an initially flat polycrystal surface to nucleate crack fronts by evaporation–condensation, subject to conditions above the threshold in the parameter space (Γ, χ, Λ).

investigation to better quantify the trends noted in this paper.

5. CONCLUDING REMARKS

Cracks may nucleate on the surface of a ceramic stressed at an intermediate temperature, where the surface changes shape by mass transport, but the bulk deforms elastically. The threshold stress depends on various basic quantities as shown in Fig. 8 for surface diffusion, and Fig. 13 for surface reaction. Everything else being fixed, the threshold stress decreases as the grain size increases according to $\sigma_{th} \propto \lambda^{-1/2}$. The crack nucleation time is given by Fig. 10 for surface diffusion, and Fig. 15 for surface reaction.

Our model makes several geometric simplifications. It assumes that the grain boundary grooves are the only geometric features on the solid surface. That is, before the stress is applied, the solid is heat treated so that imperfections (e.g., cracks, holes, and hillocks) disappear from the surface, and only grain boundary grooves survive. This surface geometry, for instance, is expected for fine-grained ceramic fibers. After the stress is applied, the model further assumes that cracks, if they do nucleate, do so along the groove roots. In reality, a crack may also nucleate on a grain surface, away from the grain boundaries. Such a crack, however, should take a longer time to nucleate than those along the groove roots. Consequently, it is reasonable to focus on cracks nucleating from the groove roots.

Common to all low dimensional models, the present models have an inherent limitation: they cannot determine the stability of a solution against a mode of perturbation not represented by the models. In particular, we do not know whether, under a small applied stress, the periodic grooves are stable against a perturbation of a wavelength longer than the grain size. The surface of a ceramic with very small grains may not be trapped by the shallow energy well, and can nucleate a crack from an imperfection of a larger length scale. This consideration would modify the threshold conditions. Under a large applied stress, the shape change is expected to localize near the groove roots, a geometry inadequately represented by the present models. Consequently, the present models overestimate the crack nucleation time. To address such issues requires models of more degrees of freedom, which we will present in subsequent papers.

Several other effects should be included in future work. Grain boundary diffusivity, even when much smaller than surface diffusivity, should relax the stress concentration near groove roots. For a ceramic of anisotropic thermal expansion (e.g. alumina), residual stress in grains should modify the threshold conditions. Surface reaction is assumed here to be the rate limiting step during evaporation; however, reactant or product diffusion in the vapor can be rate limiting. Molecular diffusivities in vapors are better understood, so that the case of vapor transport would facilitate comparison between the model and experiments.

Acknowledgements—This work was supported by NSF through grant MSS-9202165, and by an Alcoa Foundation grant.

REFERENCES

1. Readey, D. W., Lee, J. and Quadir, T., in *Sintering and Heterogeneous Catalysis, Materials Science Research*, Vol. 16, ed. G. C. Kuczynski, A. E. Miller and G. A. Sargent. Plenum Press, New York, 1984, pp. 115–136.
2. Hillig, W. B. and Charles, R. J., in *High Strength Materials*. Wiley & Sons, New York. 1965, pp. 682–705.
3. Asaro, R. J. and Tiller, W. A., *Metall. Trans.*, 1972, **3,** 1789.
4. Stevens, R. N. and Dutton, R., *Mater. Sci. Engng*, 1971, **8,** 220.
5. Chiu, C. H. and Gao, H., *Int. J. Solids Struct.* 1993, **30,** 2981.
6. Yang, W. H. and Srolovitz, D. J., *Phys. Rev. Lett.*, 1993, **71,** 1593.
7. Wang, W. Q. and Suo, Z., *J. Mech. Phys. Solids*, in press.
8. Wong, D. and Thouless, M. D., Effects of elastic relaxation on aspect ratios during island growth of isotropic films. Technical Report, Mechanical Engineering Department, University of Michigan, Ann Arbor, 1995.
9. Sridhar, N., Rickman, J. M. and Srolovitz, D. J. *Acta mater.*, submitted.
10. Suo, Z. and Wang, W., *J. appl. Phys.*, 1994, **76,** 3410.
11. Sun, B., Suo, Z. and Evans, A. G., *J. Mech. Phys. Solids*, 1994, **42,** 1653.
12. Thouless, M. D., *Acta metall. mater.*, 1993, **41,** 1057.
13. Klinger, L. M., Glickman, E. E., Fradkov, V. E., Mullins, W. W. and Bauer, C. L., *J. appl. Phys.*, 1995, **78,** 3833.
14. Srolovitz, D. J., *Acta Metall.*, 1989, **37,** 621.
15. Suo, Z., *Adv. appl. Mech.*, 1996, **33,** in press.

APPENDIX

Cycloid Geometry and Virtual Change

A cycloid is described by

$$x = (\theta + \alpha \sin\theta)R, \quad y = (\beta + \alpha \cos\theta)R, \tag{A1}$$

with θ as the variable parameter. Note that

$$\partial x/\partial\theta = (1 + \alpha \cos\theta)R, \quad \partial y/\partial\theta = -\alpha R \sin\theta. \tag{A2}$$

The length of an element of the curve, ds, is computed from

$$\partial s/\partial\theta = (1 + 2\alpha \cos\theta + \alpha^2)^{1/2}R. \tag{A3}$$

The area per period of the region between the cycloid and the x-axis is

$$\int_0^{x} y \, dx = \pi R^2(2\beta + \alpha^2). \tag{A4}$$

The unit vector normal to the element ds has components

$$n_x = -\frac{\partial y}{\partial s} = -\frac{\partial y}{\partial\theta}\frac{\partial\theta}{\partial s} = \alpha R \sin\theta \frac{\partial\theta}{\partial s} \tag{A5}$$

and

$$n_y = \frac{\partial x}{\partial s} = \frac{\partial x}{\partial\theta}\frac{\partial\theta}{\partial s} = R(1 + \alpha \cos\theta)\frac{\partial\theta}{\partial s}. \tag{A6}$$

Describe a small variation in shape and position of the cycloid by $\delta\alpha$ and $\delta\beta$. Associated with the variation, a point (x, y) on the cycloid moves by a small distance

$$\delta x = R \sin\theta\delta\alpha, \quad \delta y = R \cos\theta\delta\alpha + R\delta\beta. \tag{A7}$$

The curve element ds moves in the direction normal to the element by a distance $\delta r_n + n_x\delta x + n_y\delta y$, or

$$\delta r_n = R^2(\alpha + \cos\theta)\frac{\partial\theta}{\partial s}\delta\alpha + R^2(1 + \alpha \cos\theta)\frac{\partial\theta}{\partial s}\delta\beta. \tag{A8}$$